RSC Advances

ROYAL SOCIETY
OF CHEMISTRY

www.rsc.org/advances

Synthesis and characterization of nanocomposite polypyrrole/H-Beta zeolites for application in electrical conductivity measurement

Kai Yu[a], Narendra Kumar[a], Jorma Roine[b], Markus Pesonen[c], Ari Ivaska[a,]*

[a] *Process Chemistry Centre, Åbo Akademi University, Biskopsgatan 8, 20500, Åbo/Turku, Finland*
[b] *Industrial Physics, Turku University, Vesilinnantie 5, 20014, Åbo/Turku, Finland*
[c] *Physics, Åbo Akademi University, Porthansgatan 3,20500, Åbo/Turku, Finland*
** Corresponding author: Tel: +358 405433555, fax: +358 22154479, E-mail address: ari.ivaska@abo.fi*

Abstract

Different amount of polypyrrole (PPy) was synthesized in aqueous solution on zeolite frameworks by chemical oxidation using $FeCl_3$ as the oxidizing agent at ambient temperature (22±1 ℃). The proton form of BEA zeolites with SiO_2/Al_2O_3 ratios of 25, 150 and 300 were used as the host for PPy in this study. Both the anionic groups in zeolite structures and the chloride ions from the oxidant functioned as the dopants during the polymerization. For comparison, parallel experiments were carried out with only purified pyrrole and $FeCl_3$ in water solution in order to obtain the bulk PPy powder. Nitrogen adsorption-desorption technique, X-ray diffraction (XRD), scanning electron microscopy (SEM), transmission electron microscopy (TEM) and fourier transform infrared spectroscopy with attenuated total reflectance (FTIR-ATR) were used to characterize the composites. PPy was formed both in the inner and outer surface of the zeolite structures. The composites showed electrical conductivity at ambient temperature in the range from 6.2×10^{-6} to 1.3 S cm^{-1} depending on the ratio between pyrrole and H-Beta zeolite. Electrochemical behavior of the synthesized samples were investigated by cyclic voltammetry.

1. Introduction

Incorporation of conducting polymer into an inorganic host has been considered as an important method to generate new type of hybrid materials that have both the unique properties of semiconducting organic polymers and the mechanical strength and chemical properties of inorganic materials [1]. These composites are promising materials in catalytic applications, as well as in electronic devices due to their superior electronic, magnetic, electrical and optical properties [2-4]. Zeolites are one of the most recommended host materials due to their well-ordered pore systems that can serve as substrate for growing of conducting polymers. The anionic groups in the zeolite frameworks are expected to function as the dopants during the polymerization [5-9]. Polyaniline [10], polypyrrole (PPy) [11], polythiophene [12] and polyacrylonitrile [13] have been reported to grow in cages and channels of different zeolites both in chemical and electrochemical polymerization.

Polypyrrole is easy to synthesize by both chemical and electrochemical methods. It has a low band gap, tunable electrical conductivity, excellent environmental and thermal stability [14] and was therefore selected as the conducting polymer in the present work. In addition, the monomer size of pyrrole is small enough to enter the studied zeolite cages and channels [15].

BEA zeolite, used as the host for PPy, is an aluminosilicate microporous material with three dimensional frameworks [16]. As shown in Fig.1, the frameworks are composed by two tetragonal crystal systems: one channel consists of 12-membered rings with dimensions of 0. 56×0. 56 nm and another channel consist of 12-membered ring with dimensions of 0. 66×0. 67 nm [17]. According to the beneficial properties of BEA zeolites, such as high surface area due to high degree of open porosity and large pore size, high acidity and good thermal and chemical stability, they are generally chosen as the support for metal catalyst [18, 19]. Phani et al. reported that the SiO_2/Al_2O_3 ratio in the zeolite structure can influence the properties of conducting polymer/zeolite composite [20], therefore the proton form of BEA zeolites with SiO_2/Al_2O_3 ratio of 25, 150 and 300 were used in this work.

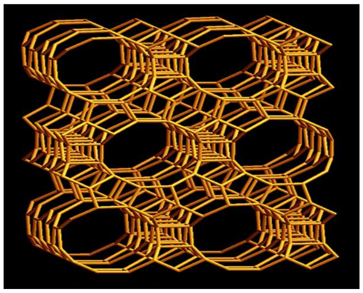

Fig. 1 Framework structure of BEA zeolites

2. Experimental

2.1 Materials

The BEA type zeolites with SiO_2/Al_2O_3 ratios of 25, 150 and 300, used as the host materials, were obtained in the NH_4-form from Zeolyst International. NH_4-Beta-25, NH_4-Beta-150 and NH_4-Beta-300 were calcined in muffale oven at 450 ℃ for four hours to generate H-Beta-25, H-Beta-150 and H-Beta-300. Pyrrole was purchased from Sigma-Aldrich (W338605 Aldrich) and distilled prior to use. The purified pyrrole was tightly sealed in argon environment and kept in dark at 0 ℃. The oxidizing agent $FeCl_3 \cdot 6H_2O$ was purchased from Sigma-Aldrich (31232 Sigma-Aldrich) and stored in desiccator as received. Deionized water was produced by system PureLAB Ultra (ELGA) for solution preparation.

2.2 Synthesis of PPy/H-Beta zeolite composite

Approx. 1.0 g H-Beta zeolite powder and 1 ml purified pyrrole were dispersed in 100 ml deionized water and stirred for 15 minutes using a magnetic stirrer. 11.0 g of $FeCl_3 \cdot 6H_2O$ was then added in the suspension. The chemical polymerization was proceeded for 24 hours in sealed glass bottle at ambient temperature (22±1 ℃). Stirring of the suspension was necessary in order to make PPy to grow evenly on the zeolite structure. Chemical polymerization of pyrrole has been described by N. V. Blinova et al [21]. Finally, the composites were filtrated and washed with deionized water and dried at 50 ℃ for 24 hours. The materials obtained were black powder composites and are denoted by 1 ml PPy/H-Beta-25, 1 ml PPy/H-Beta-150 and 1 ml PPy/H-Beta-300.

The same procedure was repeated by loading 2 ml and 3 ml of pyrrole with 1.0 g of H-Beta zeolite. The chemical compositions of the studied mixtures are summarized in Table 1.

Table 1 Selected amount of pyrrole and $FeCl_3$. $6H_2O$ [21]

Chemicals	Group 1	Group 2	Group 3
Pyrrole	1 ml	2 ml	3 ml
$FeCl_3 \cdot 6H_2O$	11.0 g	22.0 g	33.0 g

For comparison, bulk PPy powders were synthesized with the same method by loading 1, 2 and 3 ml purified pyrrole in 100 ml deionized water respectively. $FeCl_3 \cdot 6H_2O$ was used as the oxidizing agent. The schematic presentation of formation of the nanocomposite PPy/H-Beta-zeolite is given in reaction R1:

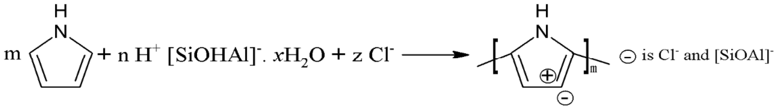

(R1)

The PPy/H-Beta composite is doped both with Cl^- and with the anionic groups $[SiOAl]^-$ in the host zeolite.

2.3 Characterization of PPy/H-Beta zeolite nanocomposite

The surface area and micropore volume of each H-Beta zeolite and the synthesized composites were determined by nitrogen adsorption-desorption technique (Sorptometer 1900, Carlo Erba) and calculated with the Dubinin-Raduskevich equation. All the samples were outgased at 150 ℃ for 3 hours before the measurements.

Scanning electron microscope (Leo Gemini 1530) having a ThermoNORAN X-ray detector was employed to study the morphology of the composite and the elemental analysis of the image was recorded at the same time. Transmission electron microscopy (JEM-1400 Plus) operated at 120 kV was used to take the micrographs of the composite samples.

Crystallinity of the composites was measured with Philips X'Pert Pro MPD X-ray powder diffractometer equipped with a Philips PW 3050/60 goniometer. The diffractometer was operated in Bragg-Brentano diffraction mode (for 2θ angle range from 4.0° to 45.0°), and the monochromatized Cu-Kα radiation was generated with a voltage of 40 kV and a current of 50 mA.

Direct current electrical conductivity measurement of the composite pellets was performed by a four point Kelvin probe setup using a Keithley 2400 Digital SourceMeter. Approx. 40 mg of the powder composite was compressed into a pellet of 10 mm diameter in a press by maintaining 4 tons of metric pressure. During the conductivity measurement a constant 10 µA bias current was applied, and the corresponding voltage through the composite pellet was determined. The measurement was repeated three times for each pellet. Finite size corrections were used to accurately calculate the conductivity of the samples using the measured current/voltage ratio.

Fourier transform infrared spectroscopy with attenuated total reflectance (FTIR-ATR) was used to analyze the molecular structure of the composite samples. The VideoMVP^{TM} ATR accessory (Harrick Scientific) mounted with a single reflection, 45^{o} angle of incidence diamond crystal was used. It was installed in a Bruker IFS66/S spectrometer employing a DTGS detector. The composites were analyzed by compressing the powder samples tightly towards the monolithic diamond crystal with sampling area of 0.2 mm^2.

Electrochemical characterizations of the synthesized components were carried out with cyclic voltammetry (CV) using the Autolab PGSTAT20 (Metrohm) connected to a conventional one-compartment three-electrode electrochemical cell in 0.1 M NaCl solution. The working electrode with surface area of 0.07 cm^2 was made in a Teflon® tube which was filled with 6 mm thickness of PPy/H-Beta composite. A glassy carbon (GC) rod was used as the counter electrode and the reference electrode was a Ag/AgCl//3M KCl electrode. For comparison, a GC/PPy electrode (surface area = 0.07 cm^2) was also prepared in 0.1 M pyrrole and 0.1 M NaCl solution under galvanostatic condition with the applied current of 0.035 mA (0.5 mA/cm^2) and reaction time of 300 seconds. Each electrode was characterized by recording cyclic voltammograms for five cycles in the potential range -0.85 V to +0.6 V with a scan rate of 1 mV/s in 0.1 M NaCl solution. The NaCl solution was first deaerated with N_2 for 15 minutes and then the N_2 gas inlet was kept above the solution during the measurement.

3. Results and discussion

3.1 Surface area and micropore volume

The surface area and the micropore volume measured by nitrogen adsorption are given in Table 2. Significant decrease both in the surface area and the micropore volume was attributed to the presence of PPy in the channels of Beta zeolites. With increasing amount of PPy the surface area and the micropore volume decreased.

Table 2 Surface area, micropore volume and conductivity of H-Beta zeolite, the composites and the pure PPy

Sample	Surface area (m^2/g)	Micropore volume ($\times10^{-3}$ cm^3/g)	Conductivity (S/cm)
H-Beta-25	520	185	5.4×10^{-9}
1 ml PPy/H-Beta-25	94	33	8.2×10^{-1}
2 ml PPy/H-Beta-25	45	16	1.2×10^{0}
3 ml PPy/H-Beta-25	25	9	2.0×10^{-1}
H-Beta-150	509	181	5.0×10^{-9}
1 ml PPy/H-Beta-150	134	48	1.3×10^{0}
2 ml PPy/H-Beta-150	21	6	1.1×10^{0}
3 ml PPy/H-Beta-150	28	6	1.4×10^{-2}
H-Beta-300	460	163	7.1×10^{-9}
1 ml PPy/H-Beta-300	52	19	6.7×10^{-1}
2 ml PPy/H-Beta-300	24	9	7.7×10^{-1}
3 ml PPy/H-Beta-300	26	9	6.2×10^{-6}
1 ml pure PPy			9.7×10^{-1}
2 ml pure PPy			1.0×10^{-1}
3 ml pure PPy			6.1×10^{-8}

3.2 Electrical conductivity measurement

The electrical conductivity of PPy/H-Beta-25, PPy/H-Beta-150 and PPy/H-Beta-300 zeolite composites with loading 1, 2 and 3 ml of polypyrrole were measured at room temperature (22±1 ℃) with the four-point probe method (Table 2). In order to study the influence of Beta zeolite host and its acidity on the electrical conductivity, pristine H-Beta-25, H-Beta-150 and H-Beta-300 zeolite were also investigated.

As can be seen in Table 2, the microporous H-Beta zeolite is an insulator. When PPy was encapsulated in the zeolite framework, the conductivity of the composite was changed from insulator to ionic conductor and further to semiconductor. With the same host zeolite the 1 ml PPy/H-Beta composite has a similar electrical conductivity as that of 2 ml PPy/H-Beta composite, however, the conductivity of the 3 ml PPy/H-Beta composite is dramatically decreased. With the same loading amount of pyrrole, the composite synthesized with H-Beta-300 zeolite exhibits a bit lower electrical conductivity than the composites with H-Beta-25 and H-Beta-150 zeolites. A higher Si/Al ratio of the host zeolite seems to have a negative effect on the electrical conductivity of the polymer-zeolite composite. This may be caused by the lower amount of Brϕnsted acid sites in the zeolite with the highest Si/Al ratio.

The electrical conductivity of pure PPy powder synthesized with 1, 2 and 3 ml of pyrrole are 9.7×10^{-1}, 1.0×10^{-1} and 6.1×10^{-8} S/cm, respectively (Table 2). The low electrical conductivity of 3 ml PPy may be due to high cross-linking in the polymer. 3 ml PPy/H-Beta zeolite composite, however, showed a much higher conductivity than that of pure PPy powder indicating that the zeolite structure has an orientating effect in formation of the polymer chains. Higher orientation of the polymer chains result also in higher electrical conductivity.

Several factors such as conjugation length and charge transfer can influence the electrical conductivity in a conducting polymer [22]. In this work, PPy immobilized in a Beta zeolite matrix exhibited enhanced electrical conductivity compared with pure PPy. Conductivities of all the composites with 1 ml loading are approximately the same as the conductivity of pure PPy. Composites with 2 ml loading, however, exhibit about ten times higher conductivity indicating better alignment of the polymer chains in the composites than in the pure PPy. When the loading is further increased to 3 ml, conductivity drops as can also be seen in the conductivity of pure PPy synthesized with the same amount of pyrrole. This shows that with high concentration of pyrrole in the synthesis of the composite the effect of the substrate, i.e., the zeolite, does not influence the degree of the order of the polymer chains as much as with lower loadings.

3.3 Scanning electron microscopy (SEM)

The morphology of the pure Beta zeolite and the PPy/H-Beta composite was studied by scanning electron microscopy (SEM). Fig. 2 shows the SEM images of pure H-Beta-25 and PPy/H-Beta-25 composites with different PPy loadings. It is observed that the shape of the crystals of pure H-Beta zeolite and PPy/H-Beta composite are circular separate and agglomerates of crystals of Beta zeolite. It can be concluded from these micrographs that modification (immobilization) of Beta zeolite by PPy does not influence the basic morphology of the Beta zeolite. The immobilization of Beta zeolite with PPy, however, influenced the average crystallite size of the Beta zeolite. The average crystallite size of pure Beta zeolite is 50-70 nm and it was smaller than that of PPy/H-Beta-25 composite, which is 80 nm (Fig. 2b-d). It can be concluded that the modification of Beta zeolite with PPy increase the average particle size. Similar increase in the crystallite size of the PPy/H-Beta-150 and PPy/H-Beta-300 composites can also be observed.

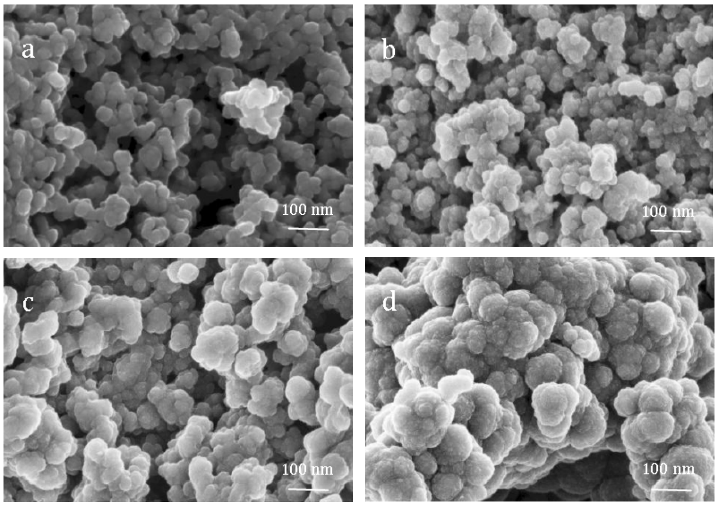

Fig. 2 Scanning electron micrographs of a) pure H-Beta-25, b) 1 ml PPy/H-Beta-25, c) 2 ml PPy/H-Beta-25 and d) 3 ml PPy/H-Beta-25

3.4 Energy dispersive X-ray analysis (EDXA)

Elemental analysis of the samples for Si, Al, N, Cl and Fe in the pure H-Beta-25, H-Beta-150 and H-Beta-300 and their PPy/H-Beta counterparts were carried out using energy dispersive X-ray microanalysis (Table 3). Pure H-Beta-25, H-Beta-150 and H-Beta-300 exhibited the presence of Si and Al. It should be pointed out that the analysis of the used H-Beta-25 and H-Beta-150 gave the same concentrations for both Al and Si. This was also confirmed by the inductively coupled plasma method. PPy/H-Beta-25, PPy/H-Beta-150 and PPy/H-Beta-300 exhibited in addition to Si and Al also N and Cl. Presence of nitrogen and chlorine are attributed to PPy and $FeCl_3$. No iron was found in the composite due to the washing procedure after the synthesis of the composite. Chlorine, however, remained in the structure due to its function as the doping anion (chloride) in the synthesis of polypyrrole.

Table 3 Elemental analysis of pure host zeolite and PPy/H-Beta composites

Sample	Si (%)	Al (%)	N (%)	Cl (%)	Fe (%)
H-Beta-25	93.6	6.4	0	0	0
1 ml PPy/H-Beta-25	33.2	2.0	54.5	10.4	0
2 ml PPy/H-Beta-25	23.0	1.5	58.1	17.4	0
3 ml PPy/H-Beta-25	15.9	1.2	59.8	24.9	0
H-Beta-150	93.6	6.4	0	0	0
1 ml PPy/H-Beta-150	31.9	2.1	49.2	15.6	0
2 ml PPy/H-Beta-150	15.8	1.1	56.7	26.5	0
3 ml PPy/H-Beta-150	11.1	0.9	60.8	27.1	0
H-Beta-300	98.8	1.2	0	0	0
1 ml PPy/H-Beta-300	35.6	0.5	51.8	12.1	0
2 ml PPy/H-Beta-300	23.8	0.4	58.2	17.6	0
3 ml PPy/H-Beta-300	18.6	0.5	60.8	20.1	0

3.5 Transmission electron microscopy (TEM)

The distribution of PPy in the host zeolite can be followed by Transmission Electron Microscopy (TEM). Fig. 3a shows the channel system of H-Beta-25 and it exhibits columnar frameworks. Fig. 3b and c present the morphology of PPy/H-Beta-25 composite. No separate zeolite nanoparticles or separate PPy clusters are observable but the host zeolite nanoparticles are rather entrapped inside the PPy clusters. Hence, the particles are glued but not mixed with the PPy. The black dots, marked by the arrows in Fig. 3c and d, belong to the PPy chains that may have been formed inside the channels of H-Beta-25 [23]. Furthermore, the decreased surface area and the micropore volume obtained for PPy/H-Beta-25, PPy/H-Beta-150 and PPy/H-Beta-300 compared with pristine H-Beta-25, H-Beta-150 and H-Beta-300 (Table 2) can be taken as a confirmation of the formation of PPy in the channels of H-Beta zeolites. In addition, the well-ordered columnar framework indicates that incorporation of PPy chains into the zeolite channels does not destroy the zeolite structure

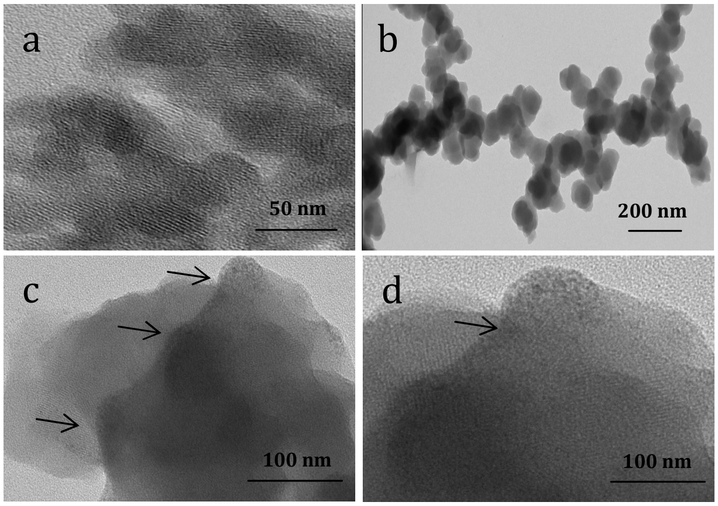

Fig. 3 Transmission electron micrographs of a) H-Beta-25, b), c) and d) 1 ml PPy/H-Beta-25 composite

3.6 X-ray powder diffraction (XRD)

The XRD diffraction patterns of pure H-Beta-25 zeolite before and after inclusion of PPy are presented in Fig. 4a. In the H-Beta-25 pattern a broad peak and a narrow peak at the 2θ values about 7.6 and 22.5 degrees are observed and they are visible also at the same positions in the PPy/H-Beta-25 patterns, indicating that the well-ordered host zeolite structure was maintained during synthesis of the composite. Compared with the pure H-Beta-25, a clear reduction in the peak intensities is observed and the more pyrrole was used in the synthesis the lower was the peak intensity in the composite diffractograms. This is caused by the relatively low scattering contrast between the pores and walls of microporous silica resulting from the PPy formation in the channels [24]. The features observed in the 1 ml PPy/H-Beta-25 XRD patterns are similar to those of 1 ml PPy/H-Beta-150 and 1 ml PPy/H-Beta-300 (Fig. 4b), however, when using H-Beta-300 as the host zeolite the obtained composite has the highest peak intensity indicating that a high Si/Al ratio will weaken the deposited amount of PPy into the zeolite framework.

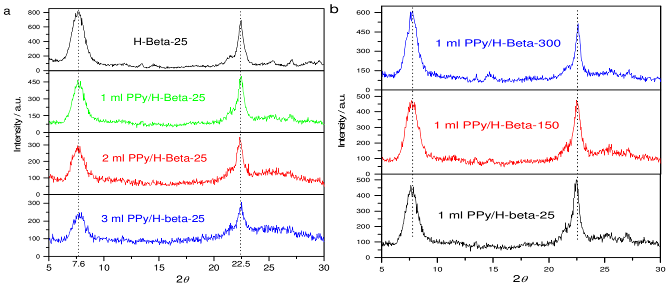

Fig. 4 XRD patterns of a) PPy/H-Beta-25 and H-Beta-25 zeolite, b) 1 ml PPy/H-Beta-25, 1 ml PPy/H-Beta-150 and 1 ml PPy/H-Beta-300

3.7 Fourier transform infrared spectroscopy with attenuated total reflectance (FTIR-ATR)

Fig. 5a shows the FTIR-ATR reflection spectra of 1 ml pure PPy, PPy/H-Beta-25 composites and their host zeolite in the region from 1800 to 850 cm^{-1}. On the pure H-Beta-25 zeolite spectrum, the peak at 1625 cm^{-1} is assigned to O-H bending vibrations of the absorbed water molecules and the typical asymmetric and symmetric Si-O-Si stretching vibrations are centered at 1228 and 1068 cm^{-1}, respectively [25, 26]. On the other hand, the spectrum of pure PPy exhibits the characteristic absorption bands at 1512 cm^{-1} (C-C and C=C stretching vibrations), 1420 cm^{-1} (C-N stretching vibration), 1264 cm^{-1} (C-H or C-N in-plane vibration) and 1074 cm^{-1} (C-H and N-H in-plane deformation vibrations) [27, 28]. These typical spectral features of pure PPy are also observable on the spectrum of 1 ml PPy/H-Beta-25 composite at 1535, 1450 and 1294 cm^{-1}. They, however, are shifted to higher wavenumbers with increasing amount of PPy in the composite (Fig. 5b). These peaks are also shifted to higher wavenumbers, though not in the same regular way, when the amount of the pyrrole monomer is increased in the synthesis of pure PPy (Fig. 5c). This indicates that the structure of the synthesized PPy is influenced by the zeolite. Generally, the C-C band tends to shift to lower wavenumbers as the conjugated length of the polymer is increased [29] and thus, the polymer chains in the PPy/H-Beta-25 composite can be considered shorter than those in the pure PPy. This can be assumed to be caused by some of the counter-ion groups in the zeolite structure replacing the Cl^- as dopants. Due to overlap with the C-H or C-N in-plane vibration (1294 cm^{-1}) and C-H and N-H in-plane deformation vibrations (1070 cm^{-1}) of the PPy, the Si-O band at 1228 and 1068 cm^{-1} of the host zeolite are not visible in the spectrum of the composite. It can therefore be assumed that PPy is formed on the framework of the host zeolite. In the chemically synthesized PPy, chloride ions function as the dopants. When the synthesis is performed in presence of zeolites, chloride ions are then also the main dopants but the anionic groups of the zeolites may also participate as dopants in the charge balance in the electrically neutral composite. A complete evaluation of the role of dopants in the composites would require more through spectra studies, also involving other spectroscopic techniques.

A comparison of the 1 ml PPy/H-Beta-25 composite spectrum with the 1 ml PPy/H-Beta-150 and the 1 ml PPy/H-Beta-300 composite spectra in Fig. 5d shows that the H-Beta zeolites with different Si/Al ratios do not have any influence on the PPy bands. It also implies that the three zeolites contain the same counter-ion groups in their frameworks.

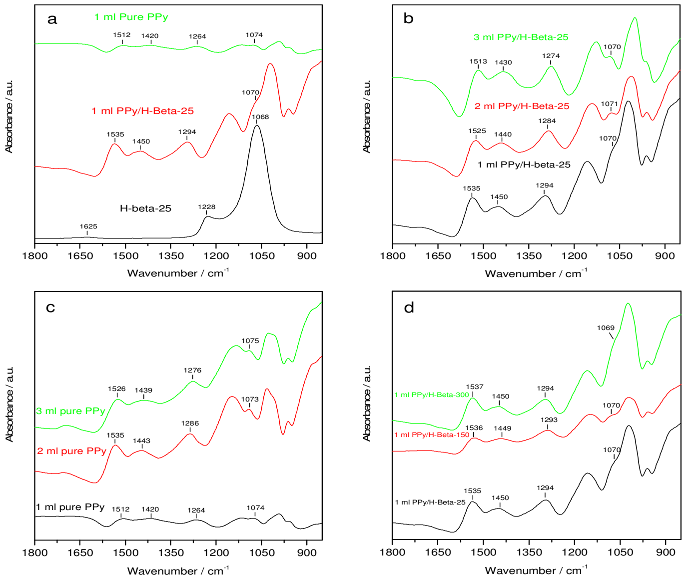

Fig. 5 FTIR-ATR spectra of a) H-Beta-25, 1 ml PPy/H-Beta-25 and 1 ml Pure PPy, b)1 ml PPy/H-Beta-25, 2 ml PPy/H-Beta-25 and 3 ml PPy/H-Beta-25, c) 1 ml pure PPy, 2 ml pure PPy and 3 ml pure PPy, d) 1 ml PPy/H-Beta-25, 1 ml PPy/H-Beta.150 and 1 ml PPy/H-Beta-300

3.8 Electrochemical characterization

Fig. 6a-c shows the cyclic voltammograms of the studied PPy/H-Beta zeolite composites and pure PPy/Cl$^-$ in 0.1 M NaCl aqueous solution at scan rate of 1 mV/s. Copared with the pure PPy/Cl$^-$, no distinct redox peaks corresponding to doping/dedoping of PPy can be found in all the composite voltammograms. All the composites curves exhibit rather resistance-like electrochemical behavior. This may be due to the compact structure of the PPy/H-Beta zeolite composites with slow doping/dedoping of PPy [30]. The differences in the cyclic voltammograms of the composite electrodes are mainly due to differences in their electrical conductivities. The 3 ml PPy/H-Beta-25 composite contains the largest amount of PPy and its CV (Fig. 6a) shows some indication of the doping/dedoping reaction of PPy.

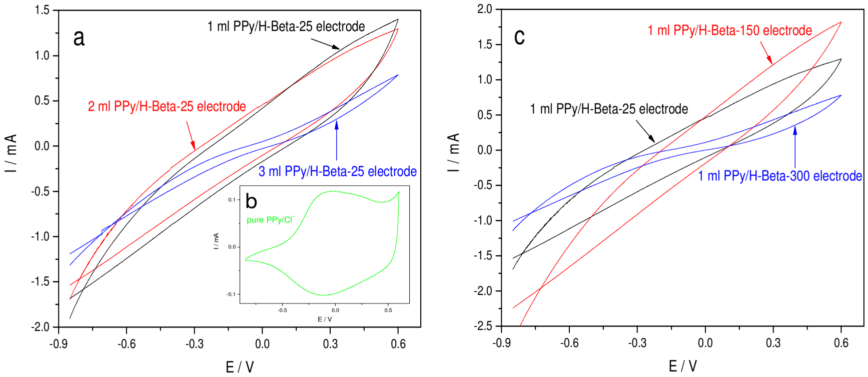

Fig. 6 Cyclic voltammograms of a) 1, 2 and 3 ml PPy/H-Beta-25 and b) pure PPy/Cl$^-$ at scan rate of 1 mV•s^{-1}, and c) 1 ml PPy/H-Beta-25, 1 ml PPy/H-Beta-150 and 1 ml PPy/H-Beta-300 at scan rate of 1 mV•s^{-1}

4. Conclusions

A series of PPy/H-Beta zeolite composites were prepared through chemical polymerization of PPy on the framework of H-Beta zeolite with Si/Al ratios of 25, 150 and 300 using FeCl$_3$ as the oxidizing agent. The surface area of PPy/H-Beta zeolite composites decreased significantly compared with that of pure H-Beta zeolite, indicating that the PPy was formed within the channels of the host zeolite structure. In addition, the surface area of the composite can be modified from hundreds to ten square meters by varying the amount of pyrrole monomer used in the synthesis reaction. SEM images showed the formation of PPy on the external surface of H-Beta zeolite. XRD patterns of PPy/H-Beta exhibited the parent structure of Beta zeolite indicating that the structure was maintained even after PPy modification. The absorption peaks in the FTIR spectrum of the pure PPy are also observed in the spectra of the PPy/H-Beta zeolite composites but at slightly lower wavenumbers. The crystallinity and nanostructure of the H-Beta zeolites were still maintained in the PPy/H-Beta composites. The increase in the conductivities in some composites compared with pure PPy may be due to increased alignment of the polymer chains in the composites. Electrical conductivity of the composites varies mainly due to the different amounts of PPy used in the polymerization. A high Si/Al ratio, i.e., low concentration of Brønsted acid sites of the host zeolite seems to have a negative effect on the electrical conductivity of the polymer-zeolite composite.

Acknowledgements

This work is part of the activities of the Åbo Akademi Process Chemistry Centre (ÅA-PCC), Finland.

Reference

1 R. Gangopadhyay and A. De, *Chem. Mater.,* 2000, **12**, 608-621.
2 T. G. Jiu, H. B. Liu, H. Y. Gan, Y. L. Li, S. Q. Xiao, H. M. Li, Y. Liu, F. S. Lu, L. Jiang and D. B. Zhu, *Synth. Met.,* 2005, **148**, 313-319.
3 H. Rein, K. Ruckpaul and W. Haberditzl, *Chem. Phys. Lett.,* 1973, **20**, 71-76.
4 A. P. Alivisators, *Science,* 1996, **271**, 933-937.
5 O. Kresnawahjuesa, G. H. Kühl, R. J. Gorte and C. A. Quierini, *J Catal.,* 2002, **210**, 106-115.
6 L. B. McCusker and C. Baerlocher, in *in Introduction to Zeolite Science and Practice,* ed. ed. J. Cejka, H. Van Bekkum, A. Corma and F. Schüth, Elsevier B.V., Amsterdam, 2007,.
7 T. Bein and P. Enzel, *Angew. Chem. Int. Ed Engl.,* 1989, **28 (12)**, 1692-1694.
8 Y. Kitayama, H. Katoh, T. Kodama and J. Abe, *Appl. Surf. Sci.,* 1997, **121/122**, 331-334.
9 G. Larsen, G. L. Haller and M. Marquez, *J Phys. Chem.,* 1992, **96**, 4145-4148.
10 P. Enzel and T. Bein, *J Phys. Chem.,* 1989, **93**, 6270-6272.
11 M. Nakayama, J. Yano, K. K. Nakaoka and K. Ogura, *Synth. Met.,* 2002, **128**, 57-62.
12 P. Enzel and T. Bein, *Synth. Met.,* 1993, **55-57**, 1238-1245.
13 P. Enzel, J. J. Zoller and T. Bein, *J Chem. Soc. Chem. Commun.,* 1992, **8**, 633-635.
14 T. J. Yao, Q. Lin, K. Zhang, H. Lv, J. H. Zhang and B. Yang, *J Colloid Interface Sci.,* 2007, **315**, 434-438.
15 G. B. Street, T. C. Clarke, R. H. Geiss, V. Y. Lee, A. Nazzal, P. Pfluger and J. C. Scott, *J Phys. Colloq.,* 1983, **C3**, 599-606.
16 C. Baerlocher, L. B. McCusker and D. H. Olson, *Atlas of Zeolite Framework Types*, Elsevier B. V., Amsterdam, 2007.
17 http://izasc.ethz.ch/fmi/xsl/IZA-SC/ftc_fw.xsl?-db=Atlas_main&-lay=fw&-max=25&STC=BEA&-find, **April 2013**.
18 J. A. Z. Pieterse, S. Booneveld and van den Brink, R. W., *Appl. Catal. B Environ.,* 2004, **15**, 215-228.
19 M. Arca, E. Arca, A. Yildiz and O. Güven, *J Mater. Sci. Lett.,* 1987, **6**, 1013-1015.
20 K. L. N. Phani, S. Pitchumani and S. Ravichandran, *Langmuir,* 1993, **9**, 2455-2459.
21 N. V. Blinova, J. Stejskal, M. Trchová, J. Prokeš and M. Omastová, *Eur. Polym. J.,* 2007, **43 (6)**, 2331-2341.
22 J. I. Kroschwitz, in *in Electrical and Electronic Properties of Polymers: A State-of-the-Art Compendium,* ed. ed. J. I. Kroschwitz, Wiley, New York, 1988, pp.1-330.
23 Q. Cheng, V. Pavlinek, C. Li, A. Lengalova, Y. He and P. Saha, *Appl. Surf. Sci.,* 2006, **253**, 1736-1740.
24 Y. Shan and L. Gao, *Mater. Chem. Phy.,* 2005, **89**, 412-416.
25 H. A. Benesi and A. C. Jones, *J. Phys. Chem.,* 1959, **63(2)**, 179-182.
26 M. L. Martinez, C. Gómez M.B., G. A. Monti and O. A. Anunziata, *Microporous Mesoporous Mater.,* 2011, **144**, 183-190.
27 C. Gómez M.B., J. M. Juarez, M. L. Martinez, A. R. Beltramone, J. Cussa and O. A. Anunziata, *Mater. Res. Bull.,* 2013, **48**, 661-667.
28 Q. Cheng, V. Pavlinek, A. Lengalova, C. Li, Y. He and P. Saha, *Microporous Mesoporous Mater.,* 2006, **93**, 263-269.
29 Y. Furulawa, S. Tazawa, Y. Fujii and I. Harada, *Synth. Met.,* 1988, **24**, 329-341.
30 J. Wang, Y. L. Xu and Sun. X.F., *Compos. Sci. Technol.,* 2007, **67**, 2981-2985.

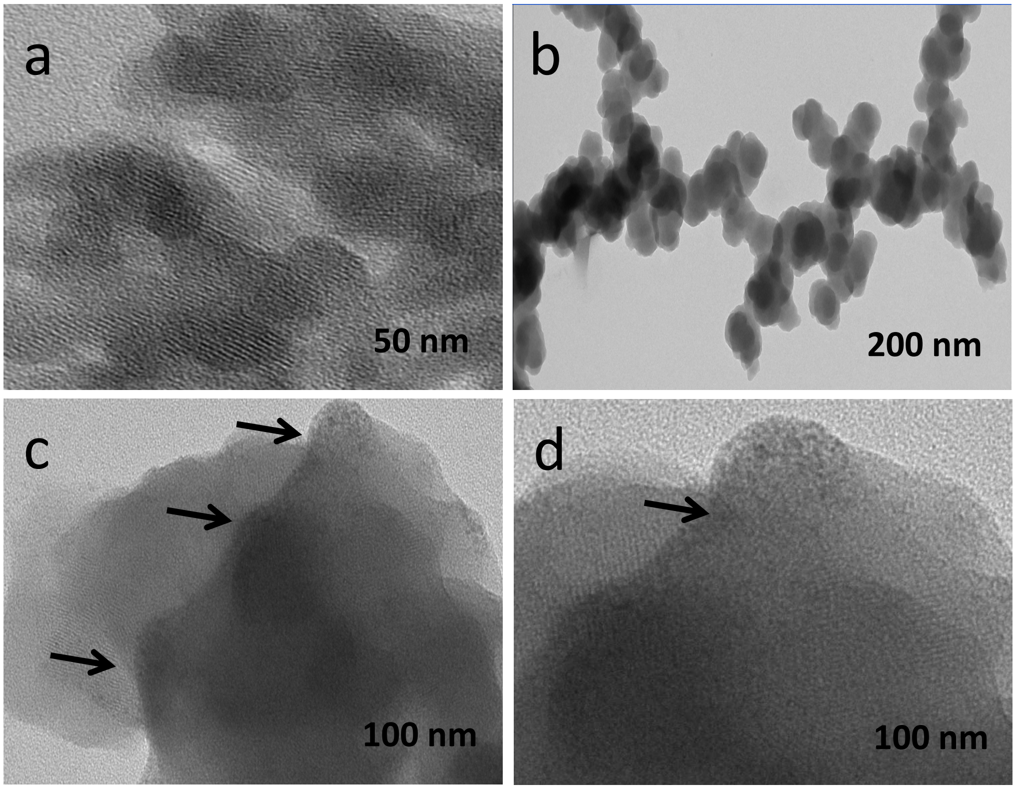

Transmission electron micrographs of a) H-Beta-25, b), c) and d) 1 ml PPy/H-Beta-25 composite